

Article

Development of Nano-Carbon Biosensors Using Glycan for Host Range Detection of Influenza Virus [†]

Toshio Kawahara ^{1,*}, Hiroaki Hiramatsu ², Yasuo Suzuki ², Shin-ichi Nakakita ³, Yasuhide Ohno ⁴, Kenzo Maehashi ⁵, Kazuhiko Matsumoto ⁶, Kazumasa Okamoto ⁷, Teruaki Matsuba ⁸ and Risa Utsunomiya ⁸

¹ College of Engineering, Chubu University, 1200 Matsumoto-cho, Kasugai, Aichi 487-8501, Japan

² College of Life and Health Sciences, Chubu University, 1200 Matsumoto-cho, Kasugai, Aichi 487-8501, Japan; hiramatu@isc.chubu.ac.jp (H.H.); suzuki@isc.chubu.ac.jp (Y.S.)

³ Life Science Research Center, Kagawa University, 1750-1 Ikenobe, Miki-cho, Kita-gun, Kagawa 761-0793, Japan; nakakita@med.kagawa-u.ac.jp

⁴ Graduate School of Science and Technology, Tokushima University, 2-24 Shinkura-cho, Tokushima 770-8501, Japan; ohno@sanken.osaka-u.ac.jp

⁵ Institute of Engineering, Tokyo University of Agriculture and Technology, 2-24-16 Nakacho, Koganei, Tokyo 184-8588, Japan; maehashi@cc.tuat.ac.jp

⁶ The Institute of Scientific and Industrial Research, Osaka University, 8-1 Mihogaoka, Osaka 567-0047, Japan; k-matsumoto@sanken.osaka-u.ac.jp

⁷ Faculty of Engineering, Hokkaido University, Kita 13, Nishi 8, Kita-ku, Sapporo, Hokkaido 060-8628, Japan; kazu@eng.hokudai.ac.jp

⁸ Nissin Electric Co. Ltd., 47 Umezu-Takase-cho, Ukyo-ku, Kyoto 615-8686, Japan; Matsuba_Teruaki@nissin.co.jp (T.M.); utsunomiya_risa@nissin.co.jp (R.U.)

* Correspondence: toshi@isc.chubu.ac.jp; Tel.: +81-568-51-9314

[†] This paper is an extended version of our paper given at the 13th International Conference on Atomically Controlled Surfaces, Interfaces and Nanostructures (ACSIN2016), Rome, Italy, 9–15 October 2016.

Academic Editors: Augusto Marcelli and Antonio Bianconi

Received: 6 October 2016; Accepted: 24 November 2016; Published: 1 December 2016

Abstract: Nano-carbon materials are promising candidates for applications in high performance devices, including highly sensitive biosensors. We have developed a self-alignment process for nano-carbon field effect transistors (FETs), using a carbon nanowall (CNW)—a nano-carbon materials—to fabricate CNW-FETs. We measured the pH dependence of the device properties. The binding molecules are known to be key components for biosensors. We are concentrating on the development of an influenza virus sensor, because the influenza virus is a major public health problem and a highly sensitive sensor is urgently required. We estimated the size of detected molecules of glycan for influenza viruses using atomic force microscopy. The typical molecule size is around 1 nm, and this may be suitable for electronic detection using a FET structure.

Keywords: self-aligned growth process for carbon nanowalls; nano-carbon biosensors; sugar chains for influenza virus detection

1. Introduction

Nano-carbon materials have enormous potential for application in advanced devices because of properties such as high mobility, high strength, and so forth [1]. They occur naturally in two-dimensional (2D) carbon sheets such as graphene [2,3]; one-dimensional carbon nanotubes (CNTs) [4] also have a carbon sheet with sp² hybridization in a cylindrical form. One of the advantages of nano-carbon materials is that field effect transistors (FETs) can be fabricated by conventional lithography. Thus, FET structures and nano-fabrication processes of nano-carbon materials could be important for certain applications. For CNTs, the carrier control of p-type and n-type conduction is also

possible using a passivation layer [5,6]. Furthermore, a single electron or hole transistor as a nano-sized device has been fabricated using nanotechnology [7] and was operational at room-temperature [8]. The carbon nanotube field effect transistor (CNT-FET) is one of the most promising candidates for use in highly sensitive sensing of gases or biomolecules. A NO₂ and Cl₂ gas sensor was reported using CNT thin films [9]. In biosensor applications, an aptamer-based novel biosensor has been developed, which can be used for the label-free detection of immunoglobulin E (IgE) protein [10,11]. We have also developed noise-enhanced nonlinear devices [12,13] and demonstrated the controllability of its operation [14–16].

Improved properties, such as for high mobility and strength, can result from the use of two-dimensional graphene sheets and application of the 2D structure itself to achieve functional nano-carbon devices. Recently, a number of researchers have concentrated on the development of nano-processes for graphene, where exfoliation of graphenes [17] and chemical vapor deposition (CVD)-grown products are used as graphene materials [1,18]. Since a metal catalyst such as copper is used for graphene growth by CVD [19], development has focused mainly on better quality transfer processes to the insulating substrates as devices. Several CVD techniques have been used by research groups [20–23]. Direct growth of graphene devices seems to be important for future electronic devices [24] and many kinds of fabrication processes have been investigated [25–30]. Graphene FETs also seem to be useful as biosensors [31] and label-free detection has been reported [32].

Carbon nanowalls (CNWs) also have such 2D structures. CNWs can be constructed by a few layers of graphene and are candidates for use as high-performance, low-dimensional materials [33]. CNWs can also be grown by the CVD technique without catalysts [34], suitable for standard semiconductor fabrication processes. Therefore, several applications have been investigated, such as using them as templates for nanostructures [35] and catalyst supports for fuel cells [36]. The control of crystallinity and carriers seems to be important in electronic device applications, and the hydrogen process [37] and nitrogen doping [38] have been proposed for quality control of CNWs. However, the position control of CNWs in the devices is difficult from the viewpoint of growth control. This represents a limitation of CNWs in applications such as transistors. As a consequence, we have developed a self-aligned process for CNWs using grapho-epitaxy [39].

Influenza is a major issue in public health [40–42]. Influenza virus A belongs to the family Orthomyxoviridae, and can easily mutate into a family of RNA viruses [43] capable of causing a change of the host range [44]. For example, the mechanism of infection of the highly pathogenic avian H5N1 influenza viruses have been studied in humans using reverse genetics [45]. The spread of influenza A virus variants needs continuous monitoring because of the high mutation rate. Many infections in humans have been reported and this might be due to the potential of these viruses to mutate and result in a change of host from birds to humans [46,47]. The surveillance of such mutations is essential, and therefore highly sensitive sensor systems are needed. We have developed a biosensor using nano-carbon materials which can detect the preferred host of the virus. The host change can be observed as a change of the bonding between the virus protein and the host sugar chain.

We have developed several processes to fabricate field effect transistors for biosensors. One is a self-alignment process using grapho-epitaxy [48] for the nano-carbon channels [49,50]. Another is a deposition process for the binding of specific molecules, such as those found in avian influenza viruses and human-type viruses [51–53]. For nano-carbon biosensors with host specificity for influenza viruses, we used sugar chains with different coordinations of terminal sialic acid and penultimate galactose, such as α 2-3 linkage sialic acid for an avian influenza virus and α 2-6 linkage sialic acid for a human virus.

In this paper, we discuss the self-alignment process and how the fabricated nano-carbon channels can recognize the ion concentration in the solution as a pH sensor [54]. Influenza virus can detect the structure of the sugar chains to infect the specific host. Therefore, we intend to use glycan as the detection molecule in the biosensor. However, the size of the molecules needs to be small for the electronic detection because of the Debye screening length. We tried to estimate the size of

sialyllactose [54], one of the candidates for detection molecules in the biosensor for influenza virus, and investigated the host specificity of sialyllactose.

2. Results and Discussion

We will initially discuss CNW-FETs. Figure 1a shows the CNW channels used as a pH sensor. The depth of the trench is 230 nm, and the CNW is grown near the corner of the trench. The CNW flake has an approximate width of 400 nm, height of 600 nm, and thickness of 10 nm. The self-aligned CNWs work as FET channels. Figure 1b shows optical microscope (OM) images. The dark pattern between the Ti/Au electrodes is the CNW channel, and the outer region of the channel was etched out using O_2 plasma.

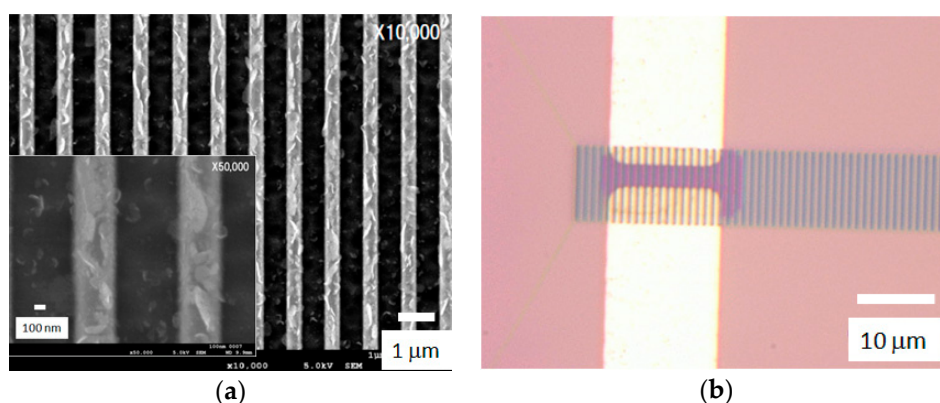


Figure 1. Representative CNW channels fabricated by the self-alignment process. (a) Scanning electron microscope (SEM) images; and (b) OM images with Ti/Au electrodes. The magnified SEM image is also shown as the inset figure.

One of the starting points for biosensors is the pH sensor, which detects ion concentration in a solution. Figure 2a shows the current-voltage (IV) characteristics of CNW-FETs at pH 4 and pH 8.2. There is a small nonlinearity; based on the metallic properties, they are the linear IV characteristics with no gate voltage dependence. This nonlinear aspect could be a result of the grain boundary scattering of carriers and shows gate voltage dependence [49]. For different pH values, the metallic part of the samples might not respond to pH, but the small change in the nonlinear part of the IV characteristics has the same tendency as CNT-FETs [55]. As shown in the inset of Figure 2a, the small change is dependent on pH. Therefore, we set the drain-source voltage (V_{DS}) to 0.2 V for the time-dependent measurements.

Figure 2b shows the time dependence of the drain-source current (I_{DS}) during the change of pH in the solution. A small drift is observed in the graph, but we can clearly observe a change of I_{DS} depending on the pH values. The nano-carbon materials therefore seem to be candidates for a biosensor. The grain boundary scattering in the flakes and the metallic feature, however, could reduce the current change.

Next, we discuss detection of molecules such as sugar chains. For electric detection in a solution, the screening length should affect the detection performance, and we therefore need to select short-length sugar chains that have a screening length approximately the same as the Debye length. Of course, the screening length can be changed by the ion concentration in the solution, but typically a few nm seems to be one of the required criteria [56].

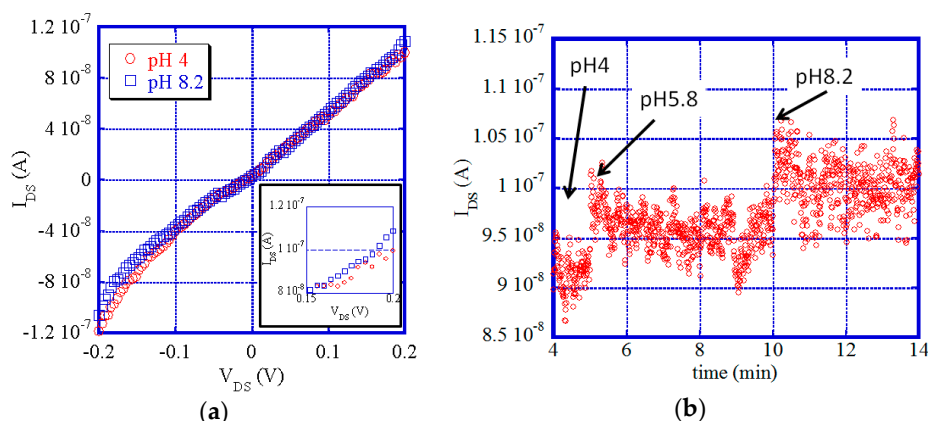


Figure 2. Representative electronic properties of the CNW-FETs in a solution. (a) Current-voltage characteristics of CNW-FETs in pH 4 and pH 8.2, and IV characteristics around $V_{DS} = 0.2$ V are enlarged as the inset figure; (b) Drain-source current change for different pH solutions.

Figure 3a shows sialyllactose molecules observed by an atomic force microscope (AFM). The concentration is 1 ng/mL. There are several molecules in the picture. Figure 3c shows the representative line profile for the molecules, indicated by an arrow in Figure 3a. The height is approximately 1 nm. These molecules appear to be suitable for use as binding molecules for the electronic detection. Figure 3b also shows an AFM image for samples with 10 ng/mL. The number of particles is higher than those in the 1 ng/mL sample and the height of the molecules is around 1 nm.

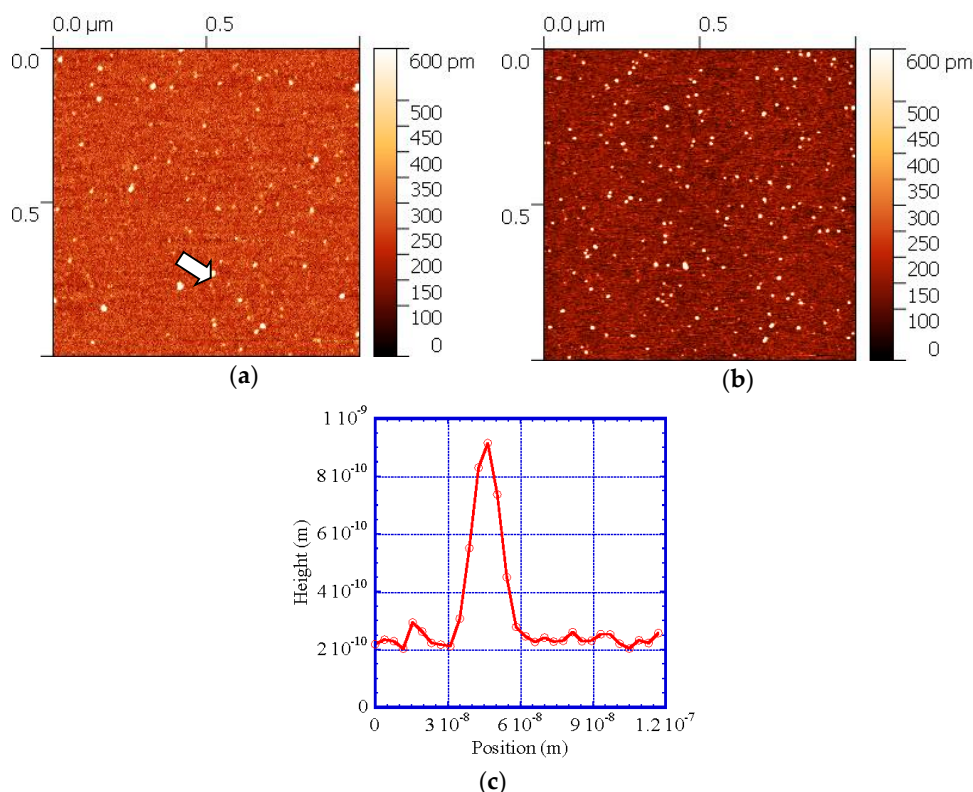


Figure 3. AFM images of sialyllactose on mica: (a) 1 ng/mL and (b) 10 ng/mL. A representative line profile for molecules indicated by an arrow in (a) is shown in (c).

Finally, we wanted to investigate the host specificity of the sugar chains to the influenza viruses. However, sialyllactose might show weak binding to the substrate, so we chose sialoglycopolymer [57]

for the enzyme-linked immunosorbent assay (ELISA) instead of sialyllactose. AFM observations confirm the small height of sialoglycopolymer and indicate the better dispersion of molecules, as shown in Figure 4. The representative line profiles in Figure 4b demonstrate that the height is also approximately 1 nm, where the height of molecules is mainly around 0.6 nm. Therefore, these molecules also seem to be suitable for use as binding molecules in electronic detection.

Figure 5 shows the binding activity of two types of influenza virus, H1N1 and H5N1, to sialoglycopolymers. H1N1 is a human-type virus and prefers to bind to α 2-6 linkage sugar chains, as shown in Figure 4a. H5N1 is an avian virus and more strongly binds to α 2-3 linkage sugar chains, as shown in Figure 4b. We further investigated this selectivity using Hemagglutinin (HA) proteins for the comparison and the same results were obtained. Therefore, our sugar chains seem to be suitable for the electronic detection of influenza viruses, and now we are developing the control of the distribution of molecules to obtain a higher sensitivity for these biosensors.

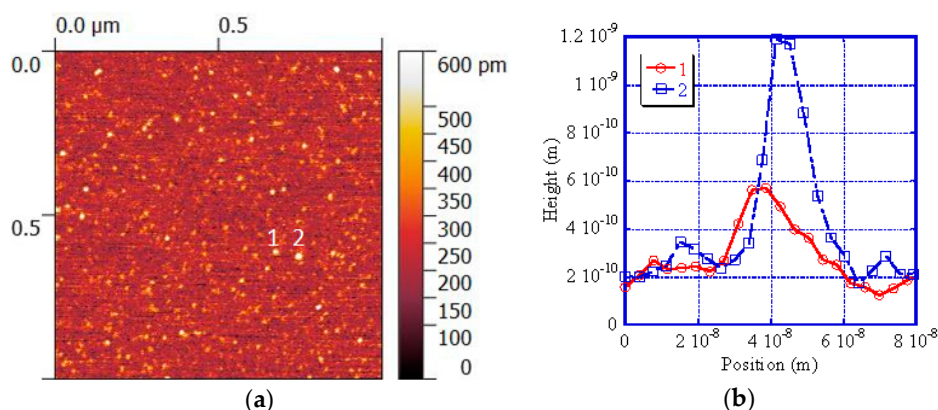


Figure 4. (a) AFM image of sialoglycopolymer on mica for 1 ng/mL. A representative line profile for molecules 1 and 2 labeled in (a) is shown in (b).

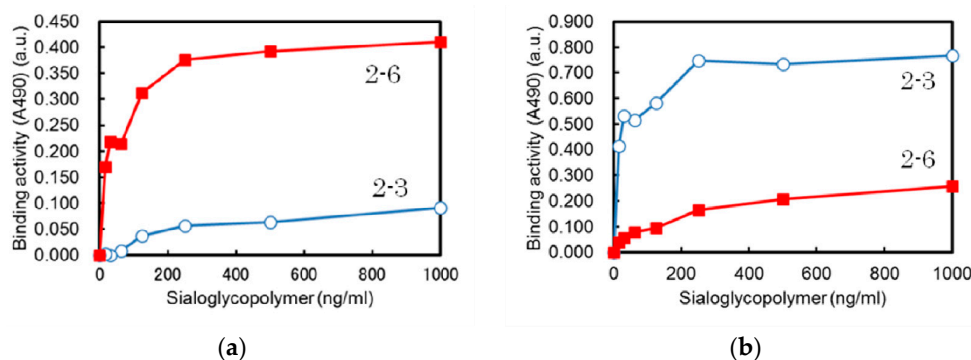


Figure 5. Binding assay of influenza viruses to sugar chains: (a) A/California/07/2009 (H1N1) and (b) A/mallard/Hokkaido/24/2009 (H5N1).

3. Materials and Methods

Si wafers with a 50 nm SiO₂ layer were used for CNW-FETs. We fabricated CNW-FETs using a self-alignment process of nano-carbon channels, one of the effective fabrication processes of nano-carbon devices. In the self-alignment process, nano-carbon materials are grown on the processed pattern on the substrate by grapho-epitaxy [48]. When suitable line and space patterns are used the surface diffusion results in self-alignment [39].

We used convex patterns of 400 nm with a concave space of 600 nm for the FET. The reactive-ion etching (RIE) time was 12 min with a plasma power of 100 W. The etched depth was typically 300 nm. For plasma-enhanced CVD growth, CH₄ gas was used as the process gas with a carrier gas of H₂.

The growth temperatures were 500 °C for 30 min. After electrode fabrication of Ti/Au, CNWs, grown outside the channel region by CVD, were etched out by O₂ plasma for 3 min with a plasma power of 100 W using photolithography.

For measurement of the pH dependence of I_{DS} of CNW-FETs, we used a top gate of an Ag/AgCl reference electrode in a 3 Mol KCl solution; to avoid a current leakage we used top gate voltage $V_g = 0$ V. V_{DS} was set to 0.2 V as stated in the previous section. We used a pH standard solutions set (HORIBA, Kyoto, Japan), which included combinations of pH = 4, 7 and 9. We first started at pH = 4, after which the other solutions were added to the small well, made of silicone rubber, on the channels of the CNW-FET. The measured pH was then 4, 5.8 and 8.2, respectively.

The glycan molecules of α 2-3 linkage sialyllactose were used for AFM observations. The powder samples of the sugar chains, which were the candidate molecules for detection, were diluted with double distilled water to 1 ng/mL or 10 ng/mL, and spread with 1 μ L on the freshly cleaved mica surface. After drying, the molecules were observed by AFM (AFM5010, Hitachi High-Tech Science, Tokyo, Japan).

In the ELISA binding assay we used the sugar chain from sialoglycopolymer, as stated in the previous section. Solutions with a concentration between 1000 and 15.6 ng/mL were spread onto 96-well plates and the 8 HAU of A/California/07/2009 (H1N1) and A/mallard/Hokkaido/24/2009 (H5N1) were fed into the wells. The HA titer, where HAU is expressed as the power of 2, is the reciprocal of the dilution that produces 1 HAU, where 1 HAU in the haemagglutinin titration is the minimum amount of virus that will cause complete agglutination of the red blood cells. We also used HA proteins for the comparison in the binding assay, namely, 500 ng/mL derived from A/California/07/2009 (H1) and A/Vietnam/1203/2004 (H5). The binding activity was measured using fluorescence at 490 nm.

4. Conclusions

We have developed a self-alignment process for nano-carbon FETs of CNWs, a promising nano-carbon material. The fabricated nano-carbon channels recognized ion concentration in solution, thereby acting as a pH sensor. To extend this work, the influenza virus can detect the structure of sugar chains to infect a specific host and we will use glycan as the detection molecule in the biosensor. However, the size of the molecules should be small for the electronic detection because of the Debye screening length. We have tried to estimate the size of sialyllactose, which is one of the candidates of detection molecules for the biosensor of influenza viruses. The size of the molecules is around 1 nm, and this seems to be suitable for electronic detection using FETs. We also investigated the host specificity of sialyllactose.

Acknowledgments: This work was supported by the Core Research for Evolutional Science and Technology (CREST), the Japan Science and Technology Agency (JST). This work was also supported by a Grand-in-Aid for Scientific Research (C) (No. 26390030) and a Grand-in-Aid for Scientific Research (B) (15H03986) under the Ministry of Education, Culture, Sports, Science, and Technology (MEXT) of Japan, and by The Science Research Promotion Fund under The Promotion and Mutual Aid Corporation for Private Schools of Japan. Part of this work was supported by the Cooperative Research Program of “Network Joint Research Center for Materials and Devices”.

Author Contributions: Toshio Kawahara, Yasuo Suzuki and Kazuhiko Matsumoto conceived and designed the experiments; Toshio Kawahara, Hiroaki Hiramatsu, Shin-ichi Nakakita, Yasuhide Ohno, Kazumasa Okamoto and Teruaki Matsuba performed the experiments; Toshio Kawahara, Kenzo Maehashi and Risa Utsunomiya analyzed the data; All authors discussed the results; Toshio Kawahara wrote the paper. All authors have read and approved the final manuscript.

Conflicts of Interest: The authors declare no conflict of interest.

References

1. Novoselov, K.S.; Fal'ko, V.I.; Colombo, L.; Gellert, P.R.; Schwab, M.G.; Kim, K. A roadmap for graphene. *Nature* **2012**, *490*, 192–200. [[CrossRef](#)] [[PubMed](#)]

2. Geim, A.K. Graphene: Status and Prospects. *Science* **2009**, *324*, 1530–1534. [[CrossRef](#)] [[PubMed](#)]
3. Fuhrer, M.S.; Lau, C.N.; MacDonald, A.H. Graphene: Materially Better Carbon. *MRS Bull.* **2010**, *35*, 289–295. [[CrossRef](#)]
4. Iijima, S.; Ichihashi, T. Single-shell carbon nanotubes of 1-nm diameter. *Nature* **1993**, *363*, 603–605. [[CrossRef](#)]
5. Kaminishi, D.; Ozaki, H.; Ohno, Y.; Maehashi, K.; Inoue, K.; Matsumoto, K.; Seri, Y.; Masuda, A.; Matsumura, H. Air-stable *n*-type carbon nanotube field-effect transistors with Si₃N₄ passivation films fabricated by catalytic chemical vapor deposition. *Appl. Phys. Lett.* **2005**, *86*, 113115. [[CrossRef](#)]
6. Maehashi, K.; Ohno, Y.; Inoue, K.; Matsumoto, K.; Niki, T.; Matsumura, H. Electrical characterization of carbon nanotube field-effect transistors with SiN_x passivation films deposited by catalytic chemical vapor deposition. *Appl. Phys. Lett.* **2008**, *92*, 183111. [[CrossRef](#)]
7. Maehashi, K.; Ozaki, H.; Ohno, Y.; Inoue, K.; Matsumoto, K.; Seki, S.; Tagawa, S. Formation of single quantum dot in single-walled carbon nanotube channel using focused-ion-beam technique. *Appl. Phys. Lett.* **2007**, *90*, 023103. [[CrossRef](#)]
8. Ohno, Y.; Asai, Y.; Maehashi, K.; Inoue, K.; Matsumoto, K. Room-temperature-operating carbon nanotube single-hole transistors with significantly small gate and tunnel capacitances. *Appl. Phys. Lett.* **2009**, *94*, 053112. [[CrossRef](#)]
9. Wongwiriyapan, W.; Honda, S.; Konishi, H.; Mizuta, T.; Ikuno, T.; Ito, T.; Maekawa, T.; Suzuki, K.; Ishikawa, H.; Oura, K.; et al. Single-Walled Carbon Nanotube Thin-Film Sensor for Ultrasensitive Gas Detection. *Jpn. J. Appl. Phys.* **2005**, *44*, L482–L484. [[CrossRef](#)]
10. Maehashi, K.; Katsura, T.; Matsumoto, K.; Kerman, K.; Takamura, Y.; Tamiya, E. Label-Free Protein Biosensor Based on Aptamer-Modified Carbon Nanotube Field-Effect Transistors. *Anal. Chem.* **2007**, *79*, 782–787. [[CrossRef](#)] [[PubMed](#)]
11. Maehashi, K.; Matsumoto, K.; Takamura, Y.; Tamiya, E. Aptamer-Based Label-Free Immunosensors Using Carbon Nanotube Field-Effect Transistors. *Electroanalysis* **2009**, *21*, 1285–1290. [[CrossRef](#)]
12. Kawahara, T.; Yamaguchi, S.; Maehashi, K.; Ohno, Y.; Matsumoto, K.; Kawai, T. Robust Noise Modulation of Nonlinearity in Carbon Nanotube Field-Effect Transistors. *Jpn. J. Appl. Phys.* **2010**, *49*, 02BD11. [[CrossRef](#)]
13. Kawahara, T.; Yamaguchi, S.; Maehashi, K.; Ohno, Y.; Matsumoto, K.; Kawai, T. Cobalt Nano Particle Size Dependence of Noise Modulations in Relation to Nonlinearity. *e-J. Surf. Sci. Nanotechnol.* **2010**, *8*, 115–120. [[CrossRef](#)]
14. Kawahara, T.; Yamaguchi, S.; Maehashi, K.; Ohno, Y.; Matsumoto, K.; Mizutani, S. Gate Voltage Control of Stochastic Resonance in Carbon Nanotube Field Effect Transistors. In Proceedings of the 2011 21st International Conference on Noise and Fluctuations (ICNF), Toronto, ON, Canada, 12–16 June 2011; pp. 364–367.
15. Kawahara, T.; Yamaguchi, S.; Ohno, Y.; Maehashi, K.; Matsumoto, K.; Mizutani, S.; Itaka, K. Diameter dependence of 1/*f* noise in carbon nanotube field effect transistors using noise spectroscopy. *Appl. Surf. Sci.* **2013**, *267*, 101–105. [[CrossRef](#)]
16. Kawahara, T.; Yamaguchi, S.; Ohno, Y.; Maehashi, K.; Matsumoto, K.; Itaka, K. Gate Voltage Dependence of 1/*f* Noise in Carbon Nanotubes with the Different Metal Contacts. In Proceedings of the 2013 22nd International Conference on Noise and Fluctuations (ICNF), Montpellier, France, 24–28 June 2013.
17. Novoselov, K.S.; Geim, A.K.; Morozov, S.V.; Jiang, D.; Zhang, Y.; Dubonos, S.V.; Grigorieva, I.V.; Firsov, A.A. Electric Field Effect in Atomically Thin Carbon Films. *Science* **2004**, *306*, 666–669. [[CrossRef](#)] [[PubMed](#)]
18. Schwierz, F. Graphene transistors. *Nat. Nanotechnol.* **2010**, *5*, 487–496. [[CrossRef](#)] [[PubMed](#)]
19. Li, X.; Cai, W.; An, J.; Kim, S.; Nah, J.; Yang, D.; Piner, R.; Velamakanni, A.; Jung, I.; Tutuc, E.; et al. Large-Area Synthesis of High-Quality and Uniform Graphene Films on Copper Foils. *Science* **2009**, *324*, 1312–1314. [[CrossRef](#)] [[PubMed](#)]
20. Nang, L.V.; Kim, E. Controllable Synthesis of High-Quality Graphene Using Inductively-Coupled Plasma Chemical Vapor Deposition. *J. Electrochem. Soc.* **2012**, *159*, K93–K96. [[CrossRef](#)]
21. Kim, J.; Ishihara, M.; Koga, Y.; Tsugawa, K.; Hasegawa, M.; Iijima, S. Low-temperature synthesis of large-area graphene-based transparent conductive films using surface wave plasma chemical vapor deposition. *Appl. Phys. Lett.* **2011**, *98*, 091502. [[CrossRef](#)]
22. Nang, L.V.; Kim, E. Low-temperature synthesis of graphene on Fe₂O₃ using inductively coupled plasma chemical vapor deposition. *Mater. Lett.* **2013**, *92*, 437–439. [[CrossRef](#)]

23. Terasawa, T.; Saiki, K. Growth of graphene on Cu by plasma enhanced chemical vapor deposition. *Carbon* **2012**, *50*, 869–874. [[CrossRef](#)]
24. Kato, T.; Hatakeyama, R. Direct Growth of Doping-Density-Controlled Hexagonal Graphene on SiO₂ Substrate by Rapid-Heating Plasma CVD. *ACS Nano* **2012**, *6*, 8508–8515. [[CrossRef](#)] [[PubMed](#)]
25. Terrones, M. Controlling the shapes and assemblages of graphene. *Proc. Natl. Acad. Sci. USA* **2012**, *109*, 7951–7952. [[CrossRef](#)] [[PubMed](#)]
26. Yamada, T.; Ishihara, M.; Hasegawa, M. Large area coating of graphene at low temperature using a roll-to-roll microwave plasma chemical vapor deposition. *Thin Solid Films* **2013**, *532*, 89–93. [[CrossRef](#)]
27. Wang, C.D.; Yuen, M.F.; Ng, T.W.; Jha, S.K.; Lu, Z.Z.; Kwok, S.Y.; Wong, T.L.; Yang, X.; Lee, C.S.; Lee, S.T.; et al. Plasma-assisted growth and nitrogen doping of graphene films. *Appl. Phys. Lett.* **2012**, *100*, 253107. [[CrossRef](#)]
28. Liao, L.; Lin, Y.; Bao, M.; Cheng, R.; Bai, J.; Liu, Y.; Qu, Y.; Wang, K.L.; Huang, Y.; Duan, X. High-speed graphene transistors with a self-aligned nanowire gate. *Nature* **2010**, *467*, 305–308. [[CrossRef](#)] [[PubMed](#)]
29. Yang, H.; Heo, J.; Park, S.; Song, H.J.; Seo, D.H.; Byun, K.E.; Kim, P.; Yoo, I.; Chung, H.; Kim, K. Graphene barristor, a triode device with a gate-controlled Schottky barrier. *Science* **2012**, *336*, 1140–1143. [[CrossRef](#)] [[PubMed](#)]
30. Wu, Y.; Jenkins, K.A.; Garcia, A.V.; Farmer, D.B.; Zhu, Y.; Bol, A.A.; Dimitrakopoulos, C.; Zhu, W.; Xia, F.; Avouris, P.; et al. State-of-the-Art Graphene High-Frequency Electronics. *Nano Lett.* **2012**, *12*, 3062–3067. [[CrossRef](#)] [[PubMed](#)]
31. Ohno, Y.; Maehashi, K.; Yamashiro, Y.; Matsumoto, K. Electrolyte-Gated Graphene Field-Effect Transistors for Detecting pH and Protein Adsorption. *Nano Lett.* **2009**, *9*, 3318–3322. [[CrossRef](#)] [[PubMed](#)]
32. Ohno, Y.; Maehashi, K.; Matsumoto, K. Label-Free Biosensors Based on Aptamer-Modified Graphene Field-Effect Transistors. *J. Am. Chem. Soc.* **2010**, *132*, 18012–18013. [[CrossRef](#)] [[PubMed](#)]
33. Wu, Y.; Qiao, P.; Chong, T.; Shen, Z. Carbon Nanowalls Grown by Microwave Plasma Enhanced Chemical Vapor Deposition. *Adv. Mater.* **2002**, *14*, 64–67. [[CrossRef](#)]
34. Tanaka, K.; Yoshimura, M.; Okamoto, A.; Ueda, K. Growth of Carbon Nanowalls on a SiO₂ Substrate by Microwave Plasma-Enhanced Chemical Vapor Deposition. *Jpn. J. Appl. Phys.* **2005**, *44*, 2074–2076. [[CrossRef](#)]
35. Wu, Y.; Yang, B.; Han, G.; Zong, B.; Ni, H.; Luo, P.; Chong, T.; Low, T.; Shen, Z. Fabrication of a Class of Nanostructured Materials Using Carbon Nanowalls as the Templates. *Adv. Funct. Mater.* **2002**, *12*, 489–494. [[CrossRef](#)]
36. Hiramatsu, M.; Mitsuguchi, S.; Horibe, T.; Kondo, H.; Hori, M.; Kano, H. Fabrication of Carbon Nanowalls on Carbon Fiber Paper for Fuel Cell Application. *Jpn. J. Appl. Phys.* **2013**, *52*, 01AK03. [[CrossRef](#)]
37. Suzuki, S.; Chatterjee, A.; Cheng, C.; Yoshimura, M. Effect of Hydrogen on Carbon Nanowall Growth by Microwave Plasma-Enhanced Chemical Vapor Deposition. *Jpn. J. Appl. Phys.* **2011**, *50*, 01AF08. [[CrossRef](#)]
38. Takeuchi, W.; Ura, M.; Hiramatsu, M.; Tokuda, Y.; Kano, H.; Hori, M. Electrical conduction control of carbon nanowalls. *Appl. Phys. Lett.* **2008**, *92*, 213103. [[CrossRef](#)]
39. Kawahara, T.; Yamaguchi, S.; Ohno, Y.; Maehashi, K.; Matsumoto, K.; Okamoto, K.; Utsunomiya, R.; Matsuba, T. Carbon Nanowall Field Effect Transistors Using a Self-Aligned Growth Process. *e-J. Surf. Sci. Nanotechnol.* **2014**, *12*, 225–229. [[CrossRef](#)]
40. Heesterbeek, H.; Anderson, R.M.; Andreasen, V.; Bansal, S.; Angelis, D.D.; Dye, C.; Eames, K.T.D.; Edmunds, W.J.; Frost, S.D.W.; Funk, S.; et al. Modeling infectious disease dynamics in the complex landscape of global health. *Science* **2015**, *347*, aaa4339. [[CrossRef](#)] [[PubMed](#)]
41. Soema, P.C.; Kompier, R.; Amorij, J.P.; Kersten, G.F. Current and next generation influenza vaccines: Formulation and production strategies. *Eur. J. Pharm. Biopharm.* **2015**, *94*, 251–263. [[CrossRef](#)] [[PubMed](#)]
42. Pillai, P.S.; Molony, R.D.; Martinod, K.; Dong, H.; Pang, I.K.; Tal, M.C.; Solis, A.G.; Bielecki, P.; Mohanty, S.; Trentalange, M.; et al. Mx1 reveals innate pathways to antiviral resistance and lethal influenza disease. *Science* **2016**, *352*, 463–466. [[CrossRef](#)] [[PubMed](#)]
43. Te Velhuis, A.J.W.; Fodor, E. Influenza virus RNA polymerase: Insights into the mechanisms of viral RNA synthesis. *Nat. Rev. Microbiol.* **2016**, *14*, 479–493. [[CrossRef](#)] [[PubMed](#)]
44. Yamada, S.; Suzuki, Y.; Suzuki, T.; Le, M.Q.; Nidom, C.A.; Sakai-Tagawa, Y.; Muramoto, Y.; Ito, M.; Kiso, M.; Horimoto, T.; et al. Haemagglutinin mutations responsible for the binding of H5N1 influenza A viruses to human-type receptors. *Nature* **2006**, *444*, 378–382. [[CrossRef](#)] [[PubMed](#)]

45. Imai, M.; Watanabe, T.; Hatta, M.; Das, S.C.; Ozawa, M.; Shinya, K.; Zhong, G.; Hanson, A.; Katsura, H.; Watanabe, S.; et al. Experimental adaptation of an influenza H5 haemagglutinin (HA) confers respiratory droplet transmission to a reassortant H5 HA/H1N1 virus in ferrets. *Nature* **2012**, *486*, 420–428. [[PubMed](#)]
46. Watanabe, Y.; Ibrahim, M.S.; Suzuki, Y.; Ikuta, K. The changing nature of avian influenza A virus (H5N1). *Trends Microbiol.* **2012**, *20*, 11–20. [[CrossRef](#)] [[PubMed](#)]
47. Watanabe, Y.; Ibrahim, M.S.; Ikuta, K. Evolution and control of H5N1. *EMBO Rep.* **2013**, *14*, 117–122. [[CrossRef](#)] [[PubMed](#)]
48. Bitai, I.; Yang, J.K.W.; Jung, Y.S.; Ross, C.A.; Thomas, E.L.; Berggren, K.K. Graphoepitaxy of Self-Assembled Block Copolymers on Two-Dimensional Periodic Patterned Templates. *Science* **2008**, *321*, 939–943. [[CrossRef](#)] [[PubMed](#)]
49. Kawahara, T.; Yamaguchi, S.; Ohno, Y.; Maehashi, K.; Matsumoto, K.; Okamoto, K.; Utsunomiya, R.; Matsuba, T.; Matsuoka, Y.; Yoshimura, M. Raman spectral mapping of self-aligned carbon nanowalls. *Jpn. J. Appl. Phys.* **2014**, *53*, 05FD10. [[CrossRef](#)]
50. Kawahara, T.; Ohno, Y.; Maehashi, K.; Matsumoto, K.; Okamoto, K.; Utsunomiya, R.; Matsuba, T. Noise spectroscopy of self-aligned carbon nanowalls. In Proceedings of the 2015 International Conference on Noise and Fluctuations (ICNF), Xi'an, China, 2–6 June 2015; pp. 108–111.
51. Ito, T.; Suzuki, Y.; Suzuki, T.; Takada, A.; Horimoto, T.; Wells, K.; Kida, H.; Otsuki, K.; Kiso, M.; Ishida, H.; et al. Recognition of *N*-glycolylneuraminic acid linked to galactose by the α 2,3 linkage is associated with intestinal replication of influenza A virus in ducks. *J. Virol.* **2000**, *74*, 9300–9305. [[CrossRef](#)] [[PubMed](#)]
52. Suzuki, Y.; Ito, T.; Suzuki, T.; Holland, R.E., Jr.; Chambers, T.M.; Kiso, M.; Ishida, H.; Kawaoka, Y. Sialic acid species as a determinant of the host range of influenza A viruses. *J. Virol.* **2000**, *74*, 11825–11831. [[CrossRef](#)] [[PubMed](#)]
53. Chandrasekaran, A.; Srinivasan, A.; Raman, R.; Viswanathan, K.; Raguram, S.; Tumpey, T.M.; Sasisekharan, V.; Sasisekharan, R. Glycan topology determines human adaptation of avian H5N1 virus hemagglutinin. *Nat. Biotechnol.* **2008**, *26*, 107–113. [[CrossRef](#)] [[PubMed](#)]
54. Bianconi, A.; Marcelli, A. (Eds.) *Atomically Controlled Surfaces Interfaces and Nanostructures*; Superstripes Press: Rome, Italy, 2016.
55. Yamamoto, Y.; Ohno, Y.; Maehashi, K.; Matsumoto, K. Noise Reduction of Carbon Nanotube Field-Effect Transistor Biosensors by Alternating Current Measurement. *Jpn. J. Appl. Phys.* **2009**, *48*, 06FJ01. [[CrossRef](#)]
56. Stern, E.; Wagner, R.; Sigworth, F.J.; Breaker, R.; Fahmy, T.M.; Reed, M.A. Importance of the Debye Screening Length on Nanowire Field Effect Transistor Sensors. *Nano Lett.* **2007**, *7*, 3405–3409. [[CrossRef](#)] [[PubMed](#)]
57. Totani, K.; Kubota, T.; Kuroda, T.; Murata, T.; Hidari, K.I.; Suzuki, T.; Suzuki, Y.; Kobayashi, K.; Ashida, H.; Yamamoto, K.; et al. Chemoenzymatic synthesis and application of glycopolymers containing multivalent sialyloligosaccharides with a poly(L-glutamic acid) backbone for inhibition of infection by influenza viruses. *Glycobiology* **2003**, *13*, 315–326. [[CrossRef](#)] [[PubMed](#)]

